Proposal to measure particle production in the Meson area using Main injector primary and secondary beams

P.D. Barnes Jr.,[3] Y. Fisyak,[1] D. Fujino,[3] E. Hartouni,[3] J. Hylen,[2] J. Morfin,[2]

C.T. Murphy,[2] A. Para,[2] R. Raja,[2*] R. Soltz,[3] S. Wojcicki,[4] D. Wright,[3] C. Wuest[3]

[1]*Brookhaven National Laboratory, Upton, NY 11973*

[2]*Fermi National Accelerator Laboratory, Batavia, Il 60510*

[3]*Lawrence Livermore Laboratory, Livermore, CA 94550*

[4]*Stanford University, CA 94305*

Abstract

We hereby submit a proposal to measure hadronic particle production with particle identification in the Meson area using primary and secondary beams from the Main Injector off a variety of targets. The purposes of the experiment are threefold; to verify a general scaling law of hadronic fragmentation, to measure particle production off a NUMI target using 120 GeV/c protons with sufficient accuracy to predict the NUMI neutrino spectrum, and to measure proton nucleus cross sections for the purposes of proton radiography. A measurement of low momentum pion production will also be of benefit to the muon collider effort.

---

*Spokesperson

Contents

I. INTRODUCTION

In what follows, we will motivate each of the aims of the experiment in some detail. We will then suggest an implementation plan for the experiment. Wherever possible, we will try to use existing equipment so as to minimize the cost and time overhead of the experiment. The key component in the experiment is a $3 million time projection chamber (EOS-TPC) built by the BEVALAC group at Berkeley. The chamber was until recently used at Brookhaven National Laboratory in the particle production experiment E-910. Further running at Brookhaven is not foreseen currently. It is important that we express an interest to secure the TPC for use at Fermilab as soon as possible in the experiment proposed herein.

II. SCALING LAW OF HADRONIC FRAGMENTATION

Even though they form more that 90% of the total inelastic cross section, very little is known about the dynamics of minimum bias interactions. The events are of such low Q^2 that perturbative QCD has little predictive power when applied to these interactions. Several scaling laws, such as KNO scaling and Feynman scaling have in the past been proposed to explain the dynamics of minimum bias interactions. These have all been shown to be disobeyed experimentally.

In 1978, a general law of scaling for inclusive reactions was proposed [1]. It was deduced heuristically, from the need to treat charged pions on an equal footing with neutral pions when extracting the annihilation cross sections by considering the difference between $\bar{p}p$ and pp cross sections. There were two Phys. Rev. D papers [2] [1]. The first shows that it is possible to estimate the annihilation component of $\bar{p}p \to \pi^0$ inclusive reactions by subtracting the corresponding $pp \to \pi^0$ component. However, this method fails for the channels $\bar{p}p \to \pi^+/\pi^-$ because of the different CP symmetry of the corresponding pp component. The situation is remedied by postulating a new equation involving charge asymmetry in $\bar{p}p$ annihilation and non-annihilation components. The new equation lets us

extract annihilation information for charged as well as neutral pions by comparing $\bar{p}p$ and pp reactions. These equations were shown to work for 12 GeV/c annihilation reactions.

The scaling law in question was proposed in order to explain the physics behind the asymmetry equation. It states that that the ratio of a semi-inclusive cross section to an inclusive cross section involving the same particles is a function only of the missing mass squared (M^2) of the system and not of the other two Mandelstam variables s and t, the center of mass energy squared and the momentum transfer squared respectively.

Stated mathematically, the ratio

$$\frac{f_{subset}(a + b \rightarrow c + X)}{f(a + b \rightarrow c + X)} \equiv \frac{f_{subset}(M^2, s, t)}{f(M^2, s, t)} = \beta_{subset}(M^2) \tag{2.1}$$

i.e. a ratio of two functions of three variables is only a function of one of them. When the subset being considered is annihilations, the asymmetry equation derived in [2] results. The physics behind the scaling law may be understood [1] by considering inclusive cross sections as the analytic continuations of crossed three body interactions, which factorize into a production term that results in the formation of a shortlived fireball of mass M^2, that subsequently decays into the subset in question. The formation is governed by s and t. The decay term is only a function of M^2. It should be noted that the physics in question falls outside the scope of perturbative QCD and as such the scaling law is not currently derivable from QCD considerations.

The law was verified in 100 GeV $\bar{p}p$ interactions by considering multiplicity subsets of the reaction $\bar{p}p \rightarrow \pi + X$. It was possible to verify the t independence of the ratio β_{subset} for a variety of subsets with an excellent degree of accuracy. The paper [1] also establishes the s independence of β_{subset} for a variety of $pp \rightarrow p + X$ reactions in the beam energy range of 200 to 400 GeV/c. Again, good agreement was obtained between the predictions of the law and data. Recently, the law has been verified in 12 reactions using data from the European Hybrid Spectrometer [3] with various beam particles and final states. Figures 1 and 2 show the test of the law for the reaction $pp \rightarrow \pi^+ + X$ for 400 GeV/c proton beam for 4 multiplicity subsets 4-6 prongs, 8 prongs, 10-12 prongs and >12 prongs. Figure 1 shows

the agreement between the predictions of the scaling law and subset data as a function of M^2 for various t ranges. Figure 2 shows the agreement between the predictions of the scaling law and subset data as a function of t for various M^2 ranges. The agreement between the predictions of the scaling law and data is excellent in the data tested so far. If the law is an exact one, as there is reason to believe it may be, then it is clearly of fundamental importance in understanding hadronic fragmentation.

The problem with existing data is that it is usually sparse as bubble chambers were being used. *It is very difficult to test the law using existing data for s independence, since only rarely has the same apparatus been used to study the same reaction at multiple energies.*

We propose to measure particle production off hydrogen and other targets as a function of beam energy for various secondary beams $(\pi^\pm, K^\pm, p, \bar{p})$, for a variety of beam momenta ranging from 5 GeV/c to 120 GeV/c. At each beam momentum, the data taking rate has to be such that approximately a million unbiased events should be recorded for analysis.

III. SYSTEMATIC ERRORS IN NUMI/MINOS MEASUREMENTS OF NEUTRINO OSCILLATION PARAMETERS

One of the methods for measuring neutrino oscillation parameters (i.e., neutrino generation mass differences and mixing angles) in the MINOS experiment is to observe a distortion in the neutrino energy spectrum observed in the "far" detector located in the Soudan mine in Minnesota. To observe such a distortion it is necessary to be able to predict with good precision the shape of the neutrino energy spectrum at Soudan in the absence of oscillations. This is done through a combination of measuring the spectrum at a "near" detector (on the Fermilab site) in concert with various NuMI beam monitoring measurements.

Monte Carlo studies have shown that the largest contributor to the systematic error in the prediction of the shape of the neutrino energy spectrum at the far detector is the uncertainty in the production spectra at the target. That is, the uncertainties in the p_T and x_F distributions of the pions and kaons produced in the target (as well as their relative
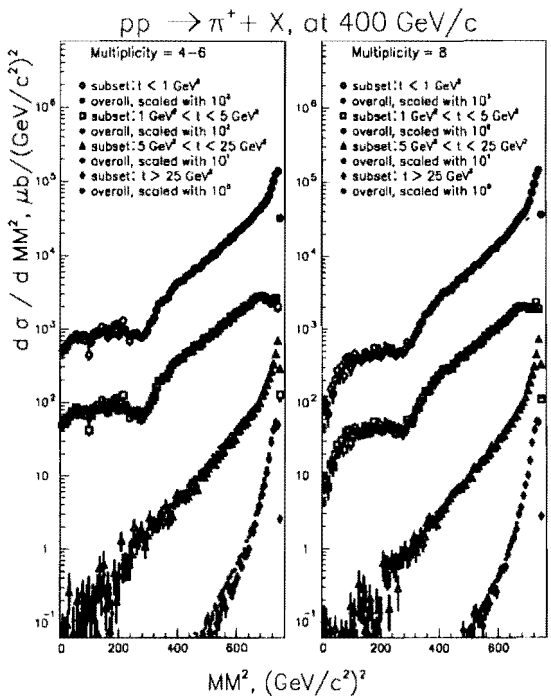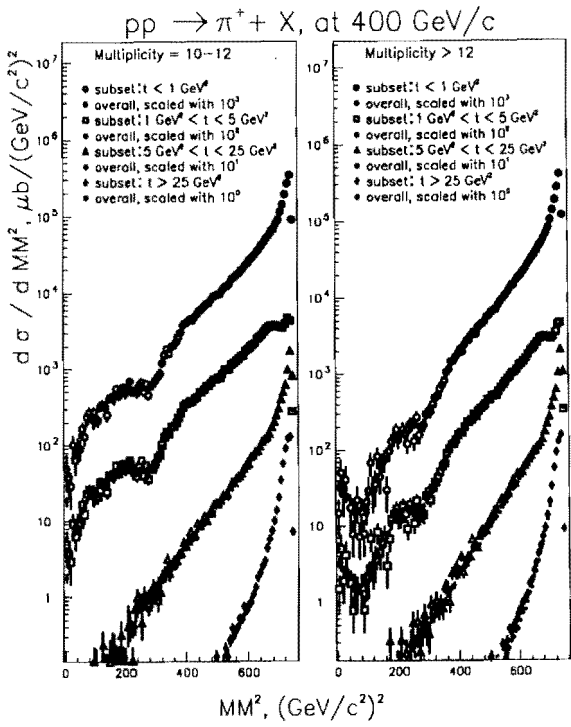
FIG. 1. M^2 distribution for the various subsets in various t ranges. Overall data, weighted by appropriate $\beta_{subset}(M^2)$ is superimposed on the subset data. Data for each t range is offset from the neighboring one by a factor of 10

6

FIG. 2. t distribution for the various subsets in various M^2 ranges. Overall data, weighted by appropriate $\beta_{subset}(M^2)$ is superimposed on the subset data. Data for each M^2 range is offset from the neighboring one by a factor of 10
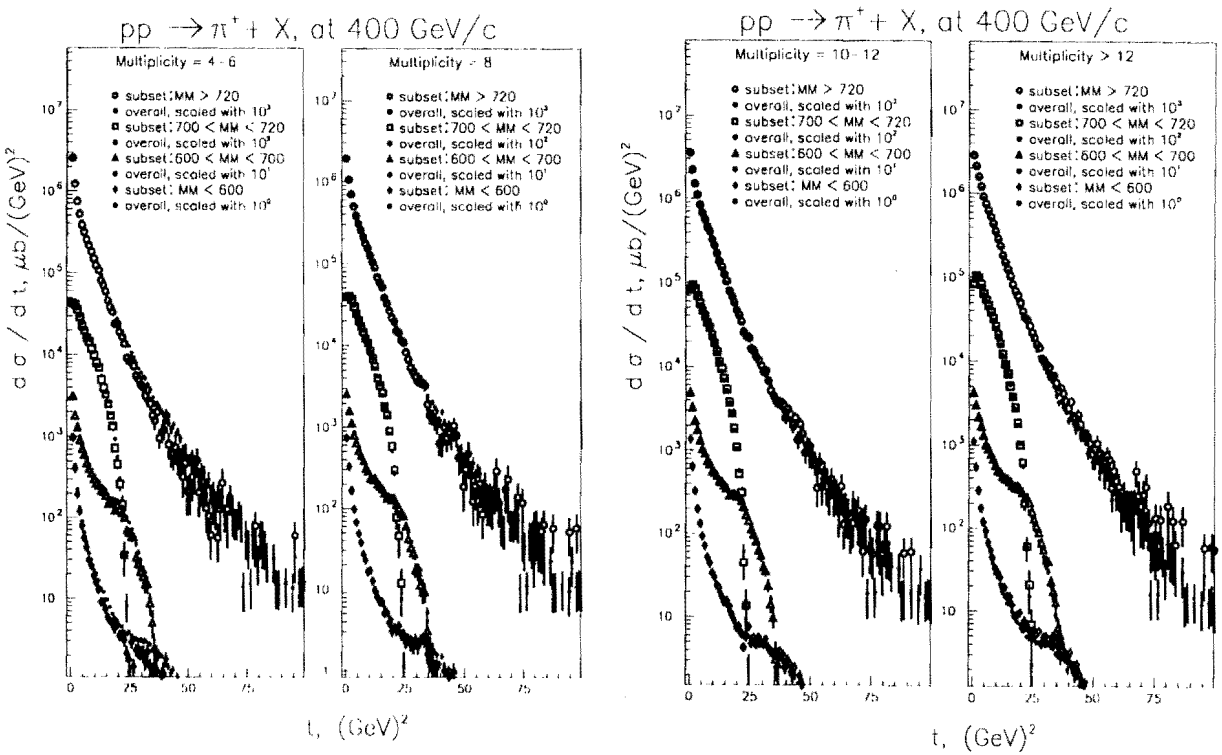
7

production rates) cannot be compensated by measurements made in the near detector. The experimental data to date on these spectra have very large statistical and systematic errors (on the order of 20%). MINOS would greatly benefit from precise experimental data on these production spectra.

In order to address the physics phase space relevant to NuMI, the following conditions need to be met:

- the beam must be 120 GeV protons from the Main Injector.

- the target must be the same as the NuMI target. Although it has not yet been finalized, the target will almost certainly be a "pencil" target (i.e., cylindrical in shape), approximately 1 to 1.5 meters in length with a radius between 1 and 5 mm.

- measurements need to be made of the p_T and x_F (or just momentum) distributions to a precision of around 2%.

- the target exit point of the hadrons needs to be measured.

- particle identification must be performed for hadrons with momentum from 5 to 80 GeV. Identification for hadrons up to 100 GeV would be useful but is not crucial.

- the forward acceptance needs to be at least 100 mrad (see Figure 3).

  The large size of the MINOS detector and the high intensity of the NUMI beam will provide a high statistics event sample. In the neutrino energy range from 8 GeV to 24 GeV, there will be of the order of 2000 charged current events per 1 GeV bin in the Soudan detector for a two year run. The detector resolution is of the order of 23%, which thus sets a natural scale of a few for detecting shape changes in the spectrum. Thus the statistical accuracy on a measurement of the energy spectrum looking for few GeV wide wiggles is between 1% and 2%. Thus a prediction of the Soudan spectrum to 1% to 2% would match the natrual statistical accuracy of the data sample. This
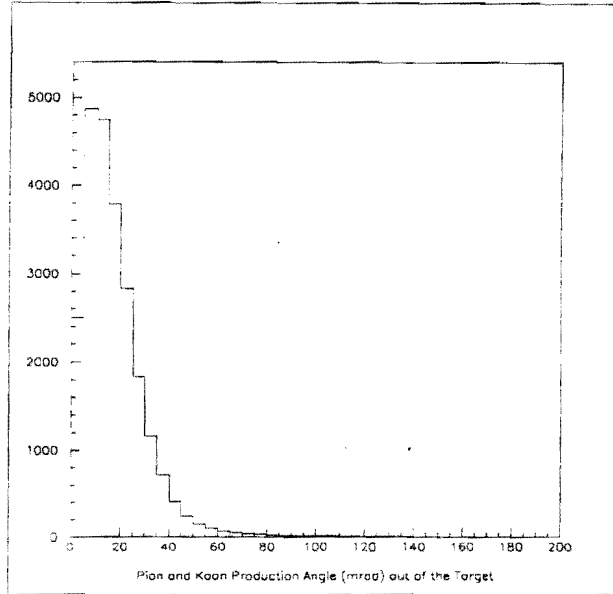
FIG. 3. The hadron production angle out of the target for NuMI.

is also the range where detector calibration will set a floor to the knowledge of the spectrum.

- measurements need to be made on K^0_S production. Presumably the p and p_T distributions can be measured using the $K^0_S \rightarrow \pi^+\pi^-$ decay channel although the exit point resolution will probably not be good enough to give useful information.

A measurement of the transverse and longitudinal momentum spectrum of pion production from the NuMI target at the 1% to 2% level would allow an absolute prediction of the neutrino spectrum in the near detector, which would serve as a powerful cross-check of the prediction of the spectrum in the far detector. A less stringent measurement, of the order of 5% in pion production, would constrain the far/near neutrino ratios to the required 2%.

To make the measurement as Monte-Carlo independent as possible, minimizing reabsorption and cascade effects, the production measurement should be done with the actual NuMI target if possible.

A large number of highly forward protons are expected, comparable to the number of pions at high momentum. It is very important to have particle identification to statistically separate these protons from the pion yield. Because the neutrino production from kaons and

9

pions is very different, particle identificaiton to statistically separate them is also important.

The bottom line is that a good measurement of the pion production from the NuMI target improves the prediction of the spectrum in the Soudan detector from about 5%-6% to about 2%, which affects the precision of the measurement of oscillation parameters, and the believability of such measurement, especially in the case of smaller neutrino mixing.

IV. PROTON RADIOGRAPHY

Currently, the Lawrence Livermore National Laboratory (LLNL) and the Los Alamos National Laboratory (LANL) are in the process of determining the feasibility of proton radiography as the radiographic probe for the Advanced Hydrotest Facility (AHF), a component of the DOE's Science Based Stockpile Stewardship (SBSS) program. The proton radiography concept would use 50 GeV/c protons to radiography thick objects with complex internal structure. One of the requirements for a successful AHF technology is the precise ($\approx 1\%$) determination of the density of these objects.

Proton radiography with high energy protons is a new technique being developed to "look" inside dense objects. A high energy beam illuminates the object. Protons undergo elastic collisions or inelastic collisions within the object depending on the material which is traversed (dependent on density, atomic number, atomic weight, reaction cross sections, etc.). The inelastic collisions which result in the loss of the proton are responsible for attenuating the incident beam. Inelastic collisions such as ionization energy loss and multiple coulomb scattering (δ-ray production) change the energy and the direction of the protons, but do not attenuate them out of the beam. The scattered beam of exiting protons is then focussed through a quadrupole lens system to an image on a detector array.

The utility of protons for radiography is related to the relatively low attenuation through thick objects, the small backgrounds on the image plane and the ability to provide multiple axes and multiple time pulses along the axes. These last two features will allow a three dimensional "movie" to be made of complex, shocked metal systems in experiments refered

to as hydrotests.

The use of protons as a radiographic probe requires a knowledge of the proton interaction cross section, the differential distribution of the outgoing proton in momentum and angle, and the distribution of produced particles, especially in the forward direction. In addition, measurements of proton interactions with a wide range of nuclei (from hydrogen to uranium) will help to quantify some of the potential difficulties in achieving high precision measurements.

There are few measurements of proton-nuclei interactions in the 50 GeV/c range. The data is especially sparse for forward particle production (see Fig. 4).
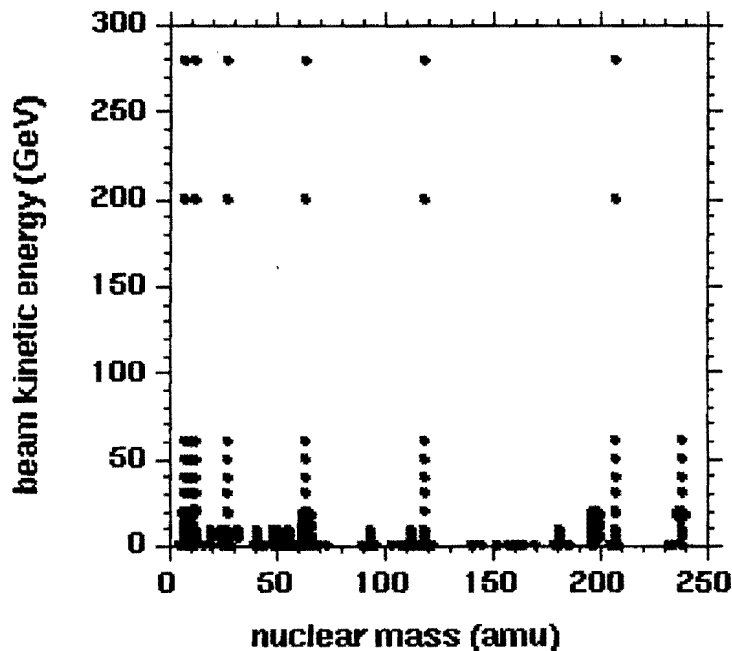

FIG. 4. This plot represents range of the world data on $pA \to X$ data as a function of beam momentum and nucleii. Each symbol represents a data point.

These data are needed to determine cross sections and particle production rates, and as input to models which will be used to generate simulated interactions for Monte Carlo studies of proton radiography.

The exact momentum of the proton beam needed for proton radiography has not yet been determined. The data obtained by this experiment should cover a wide enough range

in beam momentum to allow interpolation of data into the appropriate range for proton radiography for the materials of interest. It is likely that data spaced 10 GeV/c apart, from 5 GeV/c to 115 GeV/c would cover all of the likely range for proton radiography.

The data sets of interest consist of $\approx 10^5$ to 10^6 minimum bias interactions along with a sizable fraction of the $p + A \rightarrow p + X$ interactions (where the p is part of the "beam system"). Targets could be compatible with the scaling phase of the experiment (1% to 10% interaction lengths) and compatible triggers for the events can be established. Targets which would be of interest include: H_2, D_2, Li, Be, C, Al, Ti, Fe, Cu, Ge, Ag, Sn, W, Ta, Au, Pb, U. Target empty runs would be included as part of the cross section measurements.

Additional running with π and K beams would also provide information for particle production from the subsequent interactions of secondaries (produced in the initial pA interaction). The π and K beam particles can be identified with beam Cerenkov counters and allow for the collection of the π and K data simultaneous with the proton data.

V. MUON COLLIDER NEEDS

Measurement of the pion and kaon production cross sections of various targets is also of importance to the muon collider. The target material is not yet decided upon and the primary proton beam energy is not optimized. E910 at Brookhaven has taken data at 12.5 and 18 GeV/c primary proton momentum on beryllium, copper and gold targets, using the EOS TPC under discussion here. It would be good to repeat these measurements at beam momenta of 8 GeV/c (corresponding to the Fermilab Booster) and 30 GeV/c (corresponding to the Brookhaven AGS) on a variety of targets.

VI. IMPLEMENTATION SCHEME

Figure 5 shows the schematic of a possible experimental layout to do the proposed physics. The experiment consists of two magnetic spectrometers placed in series to cover the complete range of particle production from target to projectile fragmentation regimes

with unambiguous particle identification and excellent momentum resolution. The target, which can vary from liquid hydrogen, to various nucleii and the long NUMI target sits upstream of a time projection chamber which sits in a magnetic field supplied by the dipole magnet 1. The TPC can identify charged particles in the low energy regime by dE/dx and some resonances through their decay topology. Immediately downstream, a series of drift chambers and Cerenkov counter provide tracking and identification for the medium energy regime (1–10 GeV/c). The second spectrometer has a significantly stronger dipole magnet, a series of drift chambers, and a RICH detector, for tracking and particle identification up to the beam energies.

The precise configuration of the apparatus must await further Monte Carlo optimization. We plan to use existing apparatus where possible. Our present simulation incorporates the geometry and field of the Jolly Green Giant magnet originally of E690, and the TPL-B magnet. The Jolly Green Giant has inner dimensions of 230 x 170 x 225 cm. We assume a dipole field of 4 kGauss, yielding a p_T kick of just under 0.2 GeV/c in the configuration shown. For the TPC, inquiries have encouraged us to believe that the EOS-TPC, constructed by the BEVALAC group at Berkeley and currently installed in E895 and E910 at Brookhaven, would be available to be brought to Fermilab during the beginning of the year 1999. The TPC has dimensions of 96 x 75 x 150 cm, and consists of 128 consecutive pad-rows, each with 120 pads per row. In addition to 3D space point tracking, it provides particle identification through dE/dx. It has been quite successfully used by the E910 collaboration in the study of 18 GeV/c proton-nucleus collisions in a similar configuration. The drift chambers are modeled after the larger of the E690 drift chambers, with dimensions 180 x 120 cm, and a resolution of 200 μm. The first spectrometer also makes use of a Cerenkov counter, here taken to be the E690 counter, originally from E766, and recently a part of E910. Its x-y dimensions match the drift chambers, and it has a front mount for one chamber. The light is collected by 96 phototubes after reflection by a set of small mirrors near the center and larger ones towards the perimeter. The inner dimensions of TPL-B are 83 x 32 x 208 cm and it can run with a field of 10 kGauss for a p_T kick of approximately 1 GeV/c. For now

we show the E690 drift chambers, although slightly larger chambers would be preferable. Particle identification in the downstream spectrometer will come from a RICH detector, here taken to be the SELEX RICH, with a length of 10 m, and a diameter of 2.4 m. The chamber has been used with Neon at 1.05 atm.

We also may need to have a proton recoil detector (not shown) around the target to identify recoiling particles, such as slow protons, by time of flight. However, the TPC has demonstrated the capability to measure a significant number of the recoil target protons.
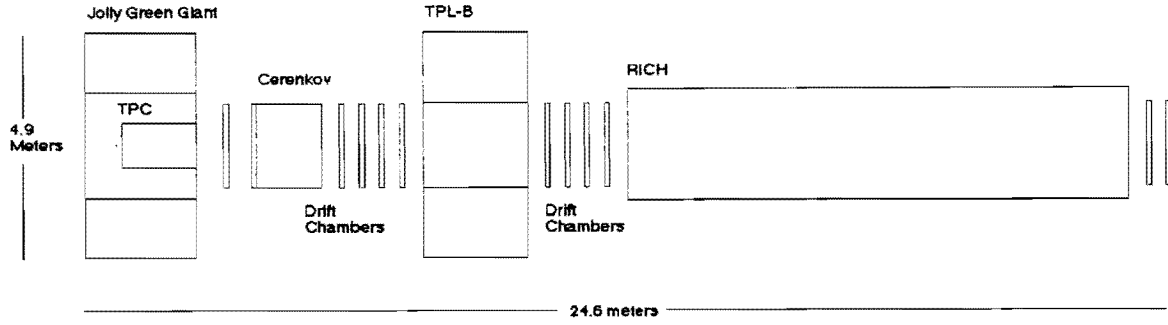

FIG. 5. Experimental layout schematic

VII. BEAM REQUIREMENTS

The primary Main Injector beam of 120 GeV/c is transported into the Meson-Polarized beam-line from the Meson-Center beam-line, Fig.6 and 7. The first two dipole dipole magnets are used to bend the beam 1.5 deg towards the experimental enclosure MP5. These two magnets can be set so that the primary beam passes by or intersects the secondary target. The target is a 2" Cu target. This target is followed by two quads, a dipole and a jaw collimator. The quads focus the secondary beam produced from the target onto the jaw collimator. The dipole disperses the beam horizontally. The jaws can be set to select a particular momentum and momentum "bite". Downstream of the jaw collimator are two additional quads and two dipoles. The quads provide a parallel beam after the focal point, and the dipoles direct the beam back into the experimental enclosure MP5. When the beam-line is run for the NuMI part of the experiment, the quads are turned off and the

14

dipoles and collimating jaws are set to allow the beam to pass to the experiment.
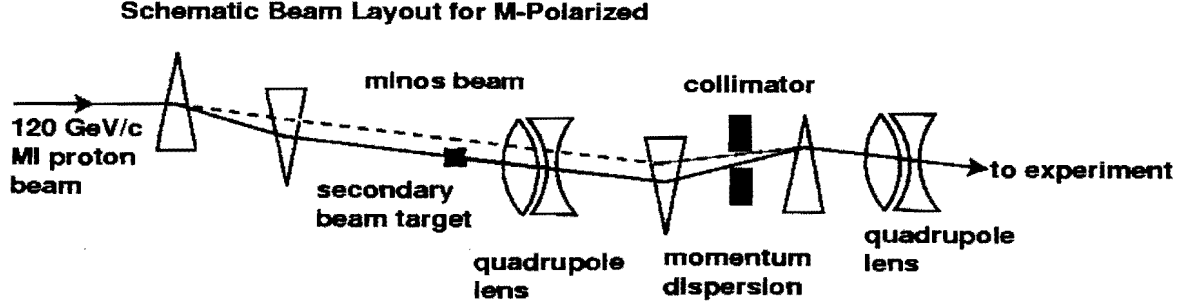
Schematic Beam Layout for M-Polarized

FIG. 6. Schematic of secondary beam-line proposed for M-Polarized.
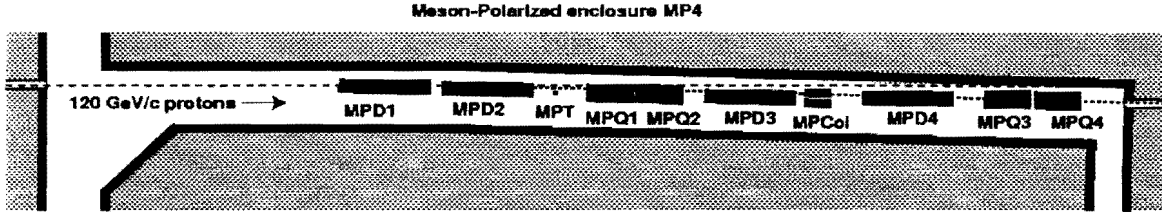

FIG. 7. Layout of proposed M-Polarized beam line in enclosure MP4.

Radiation losses will limit the beam intensities in the Meson-Polarized beam-line to less then 10^{10} protons per spill. A 2" thick Cu target is 50% of an interaction length. The secondary particle yields are shown in Figure 8 for positive particle production and in Figure 9 for negative particle production. These yields are taken from [4]. The dead time of the TPC is 16μs. The primary beam rate can be determined by the experimental requirement to obtain 10^6 unbiased events at a rate not exceeding 100 events/second. The Main Injector beam spill is 1 sec. long every 3 sec. With a 1% reaction target length, the total beam intensity at the experiment cannot exceed 10^4 particles/spill. Assuming that the total solid angle accepted by the beam-line from the target is roughly 10^{-4} the incident beam flux will be roughly $10^4/(10^{-4} \times 0.5 \times 10) = 2 \times 10^7$ protons/spill. Note however, that the π^+ and K^+ flux is greatly suppressed at high (> 80 GeV/c). With these rates, a data sample of 10^6 events can be collected in 8 hours. When running negative secondary beams the primary beam rates will have to be increased by factors of 10 to 100 to obtain comparable statistics in a similar time. The secondary beam will be tagged with two threshold gas
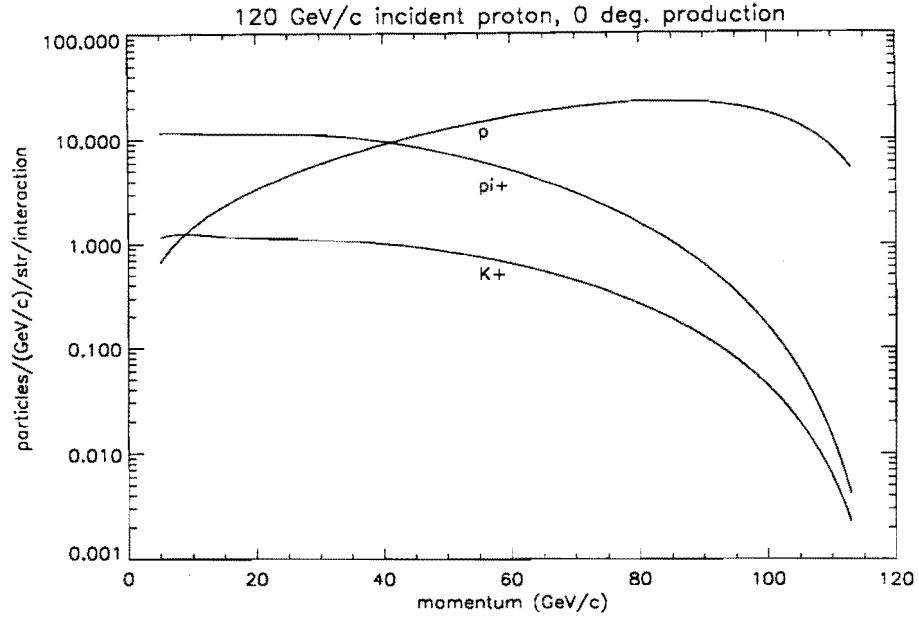
15

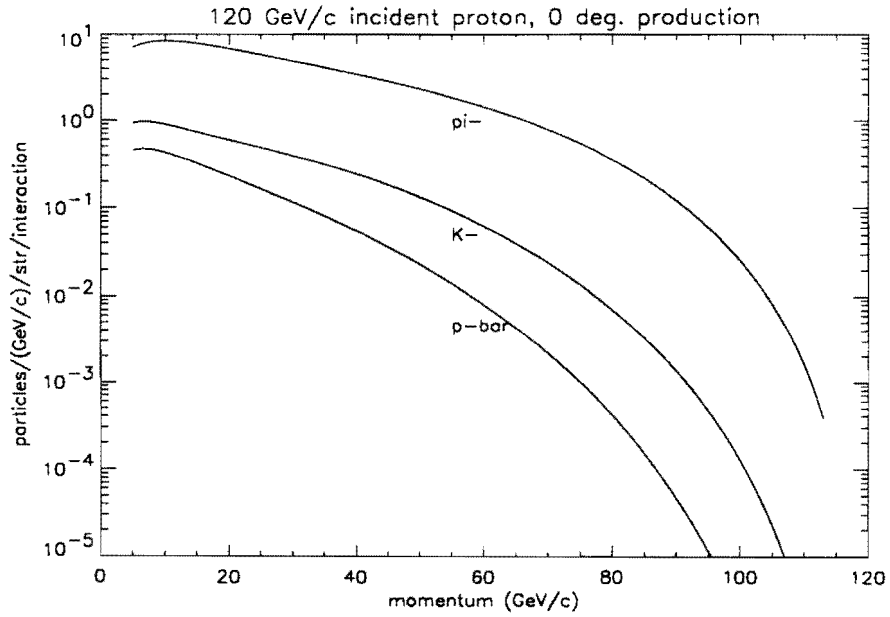FIG. 8. Positive particle production for 120 GeV/c incident proton beam from [4].

FIG. 9. Negative particle production for 120 GeV/c incident proton beam from [4].

Cerenkov counters. The three primary beam species (π,K,p) can be identified by setting the two counters so that: 1) π's radiate in counter 1, K's do not and 2) π's and K's radiate in counter 2, p's do not. The value of the index of refraction of a gas at Cerenkov radiation threshold is shown in Figures 10 and 11. These ranges of index of refractions are covered by the gases He (n=1.0000349), Ne (1.0000671), N_2 (1.000298) and CO_2 (1.000410). Additional Cerenkov counters may be required to eliminate $e^\pm$ background. Special runs will determine the $\mu^\pm$ content of the secondary beam.
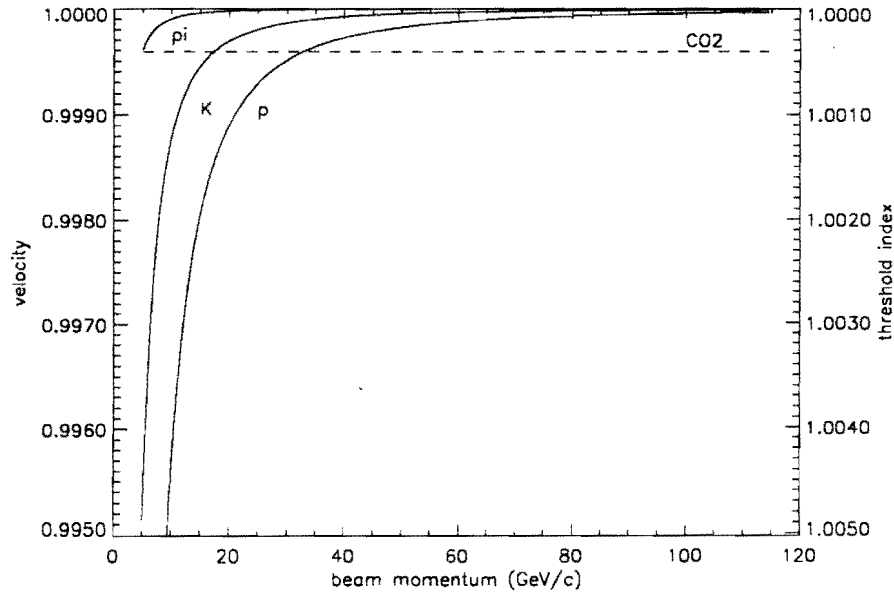

FIG. 10. Particle velocities and threshold indices of refraction as a function of secondary beam momentum.

VIII. PARTICLE ACCEPTANCE

Detector acceptances for the configuration of Figure 5 are shown in Figure 12. The four panels correspond to the following requirements:a) 10 hits in the TPC, b) a hit in the Cerenkov, c) a hit in DC 10, the drift chamber just prior to the RICH, d) passage through the mid-z-plane of the RICH. The acceptances were calculated for positive particles (protons) using a simple GEANT implementation of the proposed experimental layout. The target placement is 10 cm before the TPC front window.
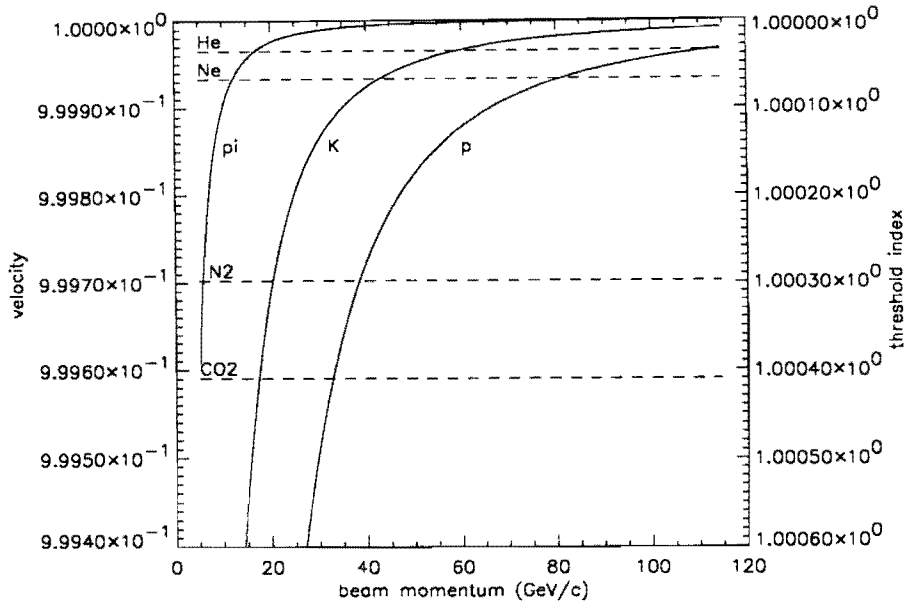
FIG. 11. Particle velocities and threshold indices of refraction as a function of secondary beam momentum.

The TPC has nearly full acceptance for particles above 0.1 GeV/c and for $\theta < 80°$, while the Cerenkov acceptance begins at 0.5 GeV/c, well below the pion threshold and for $\theta < 15°$. The second spectrometer accepts particles with $\theta < 5°$, with particles above 5 GeV/c striking the drift chamber prior to the RICH, and particles above 10 GeV/c traversing at least half of the RICH length.

We examine the worst acceptance case of the NUMI target, and simulate the acceptance assuming all particle production occurs on the front face of the target, 4 ft upstream from the nominal target placement. The results are shown in Figure 13 for the same four requirements.

The TPC acceptance is noticeably poorer, accepting particles with $\theta < 5°$ and the CKOV reduced to $\theta < 10°$. The momentum cutoffs are only slightly higher. Efficiencies in the downstream spectrometer are largely unaffected.

IX. MOMENTUM RESOLUTIONS

Using 200 μm resolution for the drift chambers, lever arms of 2 m in tracking we arrive at momentum resolutions of $\frac{\delta p}{p} = 0.05\%p$ and $\frac{\delta p}{p} = 0.01\%p$ (GeV/c) for the first and
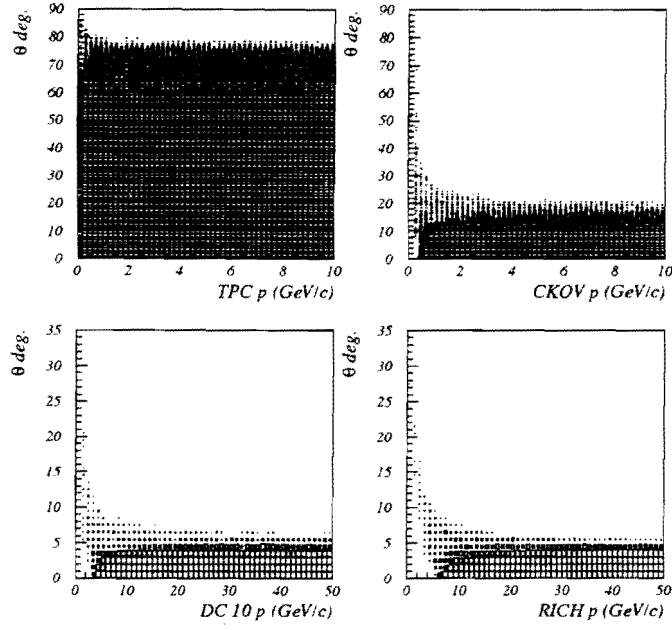
18

Positive Particle Acceptance Efficiency

FIG. 12. Acceptance Efficiencies

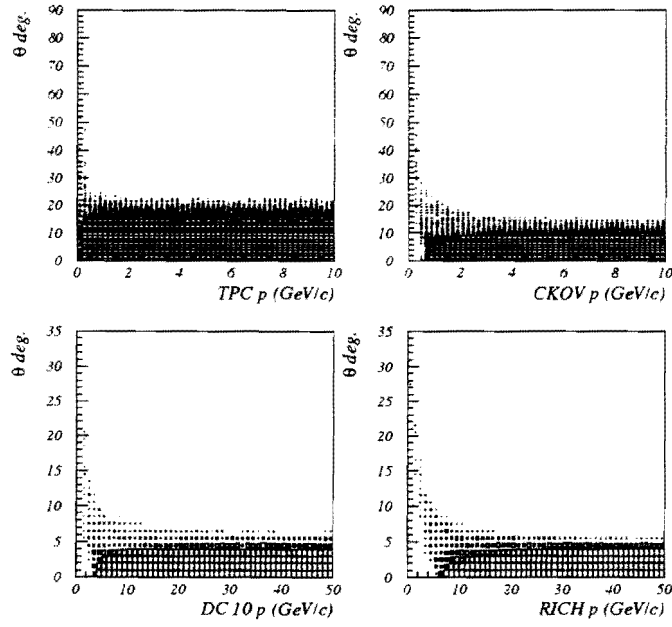*NUMI Front Acceptance Efficiency*

FIG. 13. Acceptance Efficiencies

second spectrometers respectively. Given that particles above 5 GeV/c will be measured in the second spectrometer, we expect to achieve momentum resolution below 10 MeV/c and approaching 1 MeV/c over the entire range of particle production. Simulations for the TPC in E910 also yield values which are in this range.

X. PARTICLE IDENTIFICATION

The TPC can provide 3σ separation with dE/dx up to 0.7 GeV/c for π/K and 1.1 GeV/c for K/p, as well as additional but ambiguous information in the the relativistic region. Filled with Freon 112 the Cerenkov thresholds for π, K, and p are 2.5, 7.5, and 17.5 GeV/c. The RICH detector fires at $\beta = 0.95$, and has thresholds of 0.43, 1.5, and 2.9 GeV/c.

The high end particle identification is nearly complete. Above the 7.5 GeV/c, many particles will pass through the RICH and be identified. The proton threshold is already well into the acceptance of the RICH. However, between the TPC and Cerenkov regions there is a significant gap. We will look into filling this gap with a pair of time-of-flight detectors positioned on either side of the beam line, just before the second dipole magnet. Using the current configuration the second dipole is 6 m downstream from the target. Thus, TOF capable of 100 psec. resolution would provide 3σ separation of π/K up to 2.7 GeV/c, K/p separation up to 4.6 GeV/c, nearly filling the present particle identification gap. We will continue to explore this and other possibilities.

XI. DATA ACQUISITION

The data acquisition system for this experiment is somewhat dependent on the detector systems which are identified and used. Standard CAMAC and FastBus modules can be used for a number of detector systems (e.g. the E690 Cerenkov counter, the Time-of-Flight wall, etc.). The TPC front-end communicates to a VMEbus cpu. This system could be modified to accommodate either higher speed data links (e.g. a DMA transfer from the front-end VMEbus crate to another VMEbus crate) or higher performance acquisition computers.

The Nevis electronics for the E690 chambers (includes pre-amplifiers, discriminators, TDC's and associated readout system) can be interfaced to a VMEbus system. This communication link can make use of software written for a number of Fermilab experiments which have used the Nevis data acquisition system.

All of the information can be mapped into VMEbus memory and built into an event utilizing the Fermilab Computing Division data acquisition system, DART.

XII. CONCLUSIONS

We have proposed a low cost experiment, using existing hardware, to measure particle production off hydrogen, a variety of nucleii and the NuMI target, with excellent particle identification. The quality of data thus obtained will be a significant improvement over existing measurements. The data obtained will be used to

- explore the accuracy with which a general scaling law of fragmentation is valid over a range of energy and particle type.

- measure particle production off the NuMI target with sufficient accuracy to control the systematics of measuring neutrino oscillation parameters in MINOS.

- make it possible to perform proton radiography to sufficient accuracy,

- and help pin down the choice of target material and primary beam momentum for the muon collider.

The data obtained will also help improve hadronic shower models in collider simulation programs such as Geant as well as provide a starting point for the study of the dynamics of non-prturbative QCD and its associated resonances.

XIII. COSTS

We outline below an estimate of the principal costs associated with the experiment.

Item	Estimated cost
Construction of shockproof box for transportation	$10,000
Dehumidified tent for TPC housing	$ 5,000
Transportation from BNL to FNAL	$10,000
Plumbing and electrical connections at FNAL	$10,000
Modification of the TPC optical bench	$15,000
Total estimated cost	$ 50,000

TABLE I. Estimate of costs associated with moving the TPC to Fermilab

Item	Estimated cost
Move Jolly Green Giant from Lab G to Meson	$ 50,000
New coil for Jolly Green Giant	$ 70,000
Move TPL-B from TPL to Meson	$ 50,000
Installation of magnets at Meson	$ 20,000
Total estimated cost	$ 190,000

TABLE II. Estimate of costs associated with moving magnets.

Item	Estimated cost
Recover and recommission chambers	$ 20,000
Recover and recommission data acquisition system	$ 60,000
Design and build mounting frames	$ 20,000
Purchase discriminator-to-TDC cables	$ 50,000
Total estimated cost	$ 150,000

TABLE III. Estimate of costs associated with using E690 drift chambers.

Item	Estimated cost
Move from BNL to Fermilab	$ 10,000
Design and build undercarriage system	$ 20,000
Design and build Freon recovery system	$ 20,000
Total estimated cost	$ 50,000

TABLE IV. Estimate of costs associated with using E690 Cerenkov Counter.

REFERENCES

[1] "Observation of a new regularity in hadronic spectra." R.Raja, Phys. Rev D18(1978)204.

[2] "Estimation of the annihilation component in $\bar{p}p$ interactions." R.Raja, Phys Rev D16(1977)142. This paper describes an original formula derived by me in estimating the annihilation component in $\bar{p}p$ interactions

[3] R.Raja, Y.Fisyak in Proceedings of the DPF92 meeting, Fermilab.

[4] A.Malensek, Fermilab Technical memo FN-341